Calibration of the polarization of a beam of arbitrary energy in a storage ring

R. E. Pollock, W. A. Dezarn, M. Dzemidzic, J. Doskow, J. G. Hardie, H. O. Meyer, B. v. Przewoski, T. Rinckel, and F. Sperisen
Department of Physics, Indiana University, Bloomington, Indiana 47405
and Indiana University Cyclotron Facility, Bloomington, Indiana 47405

W. Haeberli, B. Lorentz, F. Rathmann, and T. Wise
University of Wisconsin–Madison, Madison, Wisconsin 53706

P. V. Pancella
Western Michigan University, Kalamazoo, Michigan 49008
(Received 13 December 1996)

With a storage ring synchrotron, two additional methods have become possible to establish polarization standards at arbitrary energies, making use of the ease with which the energy of the stored beam can be changed. Both methods yield the analyzing power of a reaction at one energy in relation to the known analyzing power at a different energy. One method involves ramping of the energy of a polarized beam up and down; the other requires a polarized target. The two methods have been demonstrated in an experiment with the Indiana Cooler, and their relative consistency has been established. [S1063-651X(97)14706-7]

PACS number(s): 29.20.Dh, 29.27.Hj, 29.25.Pj, 13.75.Cs

I. INTRODUCTION

In a nuclear physics measurement with polarized projectiles one needs to know the absolute polarization of the beam. The beam polarization is usually determined from the scattering asymmetry in a suitable nuclear reaction for which the analyzing power is known. An example of such a polarization ''standard'' is the precisely known analyzing power in pp elastic scattering at $\theta_{lab}=8.64°$ and 183.1 MeV incident energy [1]. This standard has been derived by comparing with $^{12}C(p,p)^{12}C$ scattering at an angle and energy where the analyzing power reaches exactly unity [2]. Calibration standards are few and exist at selected energies only. It is therefore of interest to be able to extend their use to arbitrary new energies.

The beam energy in a synchrotron can be easily varied. Assuming that a polarization standard is available at one energy, T_0, a new standard can be established at a different energy, T', in one of two ways.

In method A, the beam is polarized, and the standard is used do calibrate the beam polarization at T_0. The energy of the stored beam is then increased to T' by synchrotron acceleration. If care is taken to avoid the effect of depolarizing resonances, the beam polarization should be conserved in the process. If so, the beam polarization, P, is still known at T', and an analyzing power standard $A_y(T')$ can be established at energy T' from the measured product $PA_y(T')$. In order to test that the beam polarization did not change during acceleration, the *same* beam is *de*celerated back to T_0 to remeasure its polarization by comparison with the original standard.

In method B, the roles of beam and target are reversed. The target is now polarized, and its polarization, Q, is calibrated in terms of the known analyzing power $A_y(T_0)$. Accelerating the beam does not affect the target polarization (as we will show later) and a new analyzing power standard $A_y(T')$ can be established at energy T' from the measured product $QA_y(T')$.

A comparison of the two methods is practical only if beam and target particles are identical. This is the case for the measurements reported in this paper which have been obtained during a study of spin-dependent pp elastic scattering from 200 to 450 MeV [3,4]. In Sec. II technical details related to the manipulation of the stored beam are presented. The experimental setup and the nature of the available data are described in Sec. III. Section IV contains an evaluation of the measured beam and target polarizations and a comparison of the two methods, followed by a discussion and summary in Sec. V.

II. ACCELERATION AND DECELERATION

A storage ring may function as a synchrotron accelerator if the strength of the lattice magnets increases with time as the stored beam energy is raised, through interaction with a radio-frequency cavity. The Indiana University Cyclotron Facility (IUCF) Cooler has a relatively small momentum acceptance of $\pm 0.2\%$, so the ring dipoles must match the radio frequency to a level of better than 10^{-3} during energy changes. During the course of the experiment described here, the down-ramping capability has become available at IUCF for the first time. Deceleration is possible, in principle, by time-reversing the acceleration process, however additional effort is needed to take into account such effects as the hysteresis of the ring magnets which differs between up and down ramps. Some power supplies had to be modified to cope with the energy stored in the magnets, and significant changes to the control software of the IUCF Cooler were required.

Polarized beams from the Indiana cyclotrons are kick-injected [5] into the Cooler ring at a 6.3 Hz rate. The beam is then debunched to reduce the momentum spread, decelerated

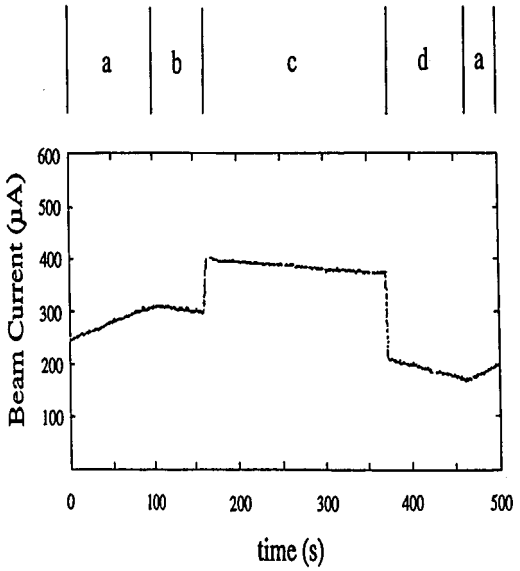

FIG. 1. Beam current versus cycle time during an acceleration-deceleration cycle. Shown are the following phases: injection (a), data taking at 197.4 MeV (b), at 399.1 MeV (c), and, again, at 197.4 MeV (d).

about 0.2% in momentum to the vicinity of the stack and cooled to add to the accumulated beam. The process can transfer about 30% of the cyclotron beam current per kick. Thus, a 1 μA cyclotron current results in a growth rate of stored current of about 100 μA/min. During injection, the beam manipulations require most of the momentum aperture, so the dispersion at the target cell (see below) must be less than about 0.5 m to avoid a degradation of the injection efficiency.

Given a nominal field ramp rate of 0.5 to 1 Tm/s, the acceleration lasts typically 1 to 3 s. The rf cavity used for stacking is also used for acceleration, with the voltage raised from about 15 to 150 V while the ramp is in progress. During deceleration, the beam momentum is reduced at the same rate as for acceleration. The lower energy may be chosen to match the injection energy, so that the remaining beam is retained for further accumulation.

Each of the steps in the acceleration-deceleration cycle (see Fig. 1) may be judged from the standpoint of the surviving fraction of beam current (transmission) and of beam polarization. Transmissions measured during individual up- and down-ramps may exceed 98%, while beam survivals in excess of 90% have been observed for the full cycle. In other words, beam losses due to ramping are comparable to those due to the lifetime during the data acquisition periods.

The beam polarization survival during an acceleration-deceleration cycle is sensitive to the choice of the initial betatron tune. This is because at the injection energy of 200 MeV, the tune ν_y is closest to matching the condition for the intrinsic depolarization resonance that satisfies $G\gamma=7-\nu_y$, where $G=1.793$ is the anomalous magnetic moment of the proton. If the fractional part of the tune is separated from the resonant tune by more than 0.03 the injected beam stays polarized. It is then sufficient to ensure that the ring tunes do not change rapidly as acceleration starts or deceleration ends. Elsewhere in the ramp cycle the beam is far from the depolarization resonance and exact control of tunes is no longer necessary. The measurement of the tune is achieved by exciting a small-amplitude betatron oscillation within the machine acceptance. The horizontal and vertical beam positions are measured on a turn-by-turn basis, and a fast Fourier transform is performed at a rate of 10 Hz, yielding a real-time measurement of the coherent betatron fractional tune [6].

III. EXPERIMENTAL DETAILS

A. Apparatus

The data reported here have been obtained during a measurement of spin-correlation parameters in pp elastic scattering from 200 to 450 MeV [4]. Apart from a few modifications, the apparatus is the same as that used in a previous measurement of pp elastic scattering at the fixed energy of 197.8 MeV [3]. Forward-going protons are detected by a set of wire chambers and scintillator arrays, while the associated recoil protons are observed in coincidence by an array of semiconductor detectors, mounted close to the target. The detection of pp coincidences provides a clean signature for pp scattering [an estimate of the background yields $(0.2\pm0.2)\%$ [3]]. From the measured direction of the forward proton, the scattering angles θ and ϕ are determined. Data are accepted within a range $\Delta\phi=\pm18°$ in four azimuthal directions ϕ (45°, 135°, 225°, 315°). Thus, for each θ angle bin and each choice of beam and target polarization direction, four yields are measured. From the observed yields, polarization asymmetries are extracted by the ''diagonal scaling method'' [3].

The polarized internal hydrogen target consists of a thin-walled storage cell into which a beam of polarized atoms is injected [7,8]. A guide field, generated by coils outside the vacuum chamber, determines the target polarization direction which can be either sideways, vertical or along the beam direction. When the current in the guide field coils is reversed, the sign of the target polarization changes within about 50 ms.

The beam polarization is vertical. The injected polarization is chosen to point either up or down. In addition, the sign of the polarization of the stored beam can be changed rapidly by crossing an artificial depolarizing resonance, induced by a longitudinal, rf magnetic field [9,10].

Thus, there are 12 possible combinations of beam and target polarization (''spin states''). Data are accumulated for these spin combinations in a sequence in which the target polarization changes every 2 s, and the beam polarization about every 15 min.

B. Data analysis

The direction of the forward protons is known from wire chamber information. The events that satisfy the conditions for pp elastic scattering are sorted into 1° bins of the laboratory scattering angle θ which ranges from 8° to 43°. From the observed yields, accumulated in 12 different spin states, polarization asymmetries are extracted by the ''diagonal scaling method'' which is described in detail in Ref. [3]. This results in the asymmetries $PA_y(\theta_i)$, $Q_xA_y(\theta_i)$, and $Q_yA_y(\theta_i)$, where $A_y(\theta_i)$ is the analyzing power for the ith θ

bin (note, that the analyzing power is the same for polarized beam or polarized target), and P, Q_x, and Q_y are the magnitudes of the beam polarization and the horizontal and vertical target polarizations, respectively. It is known [3] that the magnitude of the target polarization does not depend on the direction of the guide field. Thus, the information for the two target orientations is combined into a target asymmetry $QA_y(\theta_i)$. Data acquired with longitudinal target polarization are not used in the context of this paper.

C. Structure of an experimental cycle

An internal-target experiment typically consists of repetitions of a set of manipulations, called a ''cycle.'' In the present case, a cycle is organized as follows (see Fig. 1). First, protons from a polarized ion source are accelerated in the cyclotron to $T_0=197.4$ MeV and accumulated in the Cooler ring (see Sec. II). When the filling process is completed, after a few seconds of cooling, the beam of polarized atoms is admitted to the target cell, and data taking is enabled. During the data period which follows, the target polarization changes direction and sign in 2 s intervals, for a full ''subcycle'' of 12 s duration. After two such subcycles, the beam energy is ramped to T', and the subcycles are resumed for the measurement at the higher energy. After 6 subcycles at T', the beam is decelerated back to the injection energy T_0, where another 3 subcycles of data are taken. To identify the three data taking periods, we choose the nomenclature ''PRE'' and ''POST'' for the two measurements at T_0, before and after the two energy ramps, and ''HE'' for the measurement at the higher energy T'. The next cycle is started with beam injection, adding to the beam which is still stored. At the beginning of each cycle, the sign of the polarization of the injected beam, as well as that of the beam remaining in the ring, is reversed.

D. Polarization standard

In this measurement we make use of the fact that the absolute analyzing power is known at the injection energy $T_0=197.8$ MeV for $\theta_{\rm lab}$ from 4° to 17° from a previous experiment [3]. In that experiment, we made use of the analyzing power standard in pp scattering [1] mentioned in Sec. I. For the following, we define a secondary standard $a_j^{\rm cal}=A_y(\theta_j,197.8\ {\rm MeV})$ to be the values of the analyzing power in 1° bins for the above angular range as obtained in the previous experiment [3]. The absolute normalization uncertainty of these analyzing powers is $\pm 1.3\%$. Details about the derivation of the normalization can be found in Ref. [3]. The 0.4 MeV difference in bombarding energy between the previous and the present experiment is ignored.

IV. MEASUREMENTS

A. Definitions

During the week of running time which yielded the present data, the spin correlation coefficients A_{xx}, A_{yy}, and A_{xz} in pp scattering were measured at seven different energies. Effectively, this means that the ring operators used seven different setups for the up and the down ramp of the ring magnet currents, corresponding to the final energies T' of 250, 280, 295, 310, 350, 400, and 450 MeV. The six lower energies were measured during a single running period, while data at 450 MeV were the subject of a separate run, earlier by about a month. As mentioned before, data were accumulated before the energy ramp (''PRE''), at the higher energy T' (''HE''), and after the down ramp (''POST'').

The results presented here are deduced from ratios between angular distributions of the beam and target asymmetries $p_i=PA_y(\theta_i)$, and $q_i=QA_y(\theta_i)$. We define the ratio $\xi\equiv\{\alpha_i\|\beta_i\}$ between two distributions α_i,β_i (with errors $\delta\alpha_i,\delta\beta_i$) to be the number ξ that minimizes the function $\chi^2(\xi')$, given by

$$\chi^2(\xi')=\sum_{i=1}^{n}\frac{(\alpha_i-\xi'\beta_i)^2}{\delta\alpha_i^2+(\xi'\delta\beta_i)^2}. \tag{1}$$

The uncertainty $\delta\xi$ is determined by applying the Gauss law for error propagation.

For the following, we introduce the abbreviation $\{p_i^m\|q_i^k\}$ for the ratio between $p_i=PA_y(\theta_i)$ measured during data period m, and $q_i=QA_y(\theta_i)$ measured during data period k. For example, $\{p_i^{\rm PRE}\|q_i^{\rm PRE}\}$ is the ratio between the beam and target asymmetries, both measured before the energy ramp. Since the analyzing powers in the elements of the two distributions are the same, it is easy to see that the experimental $\{p_i^{\rm PRE}\|q_i^{\rm PRE}\}$ equals the ratio of beam and target polarization $P^{\rm PRE}/Q^{\rm PRE}$, independent of the analyzing power of the reaction.

B. Target polarization

We have mentioned that the target polarization can be assumed to be constant over a full cycle, i.e., the same at T_0 and at T'. In fact, the target polarization was constant during the whole run which lasted about one week. Since the values $a_j^{\rm cal}$ of the analyzing power at the injection energy are known (see Sec. III D), we can determine the target polarization before and after the two ramps from the ratios $\{q_j^{\rm PRE}\|a_j^{\rm cal}\}$ and $\{q_j^{\rm POST}\|a_j^{\rm cal}\}$. The average target polarization $\langle Q^{\rm PRE},Q^{\rm POST}\rangle$ and the difference $Q^{\rm POST}-Q^{\rm PRE}$ measured in this way are shown in Fig. 2 as a function of run number, or time during the run. Since the calculated weighted average for the difference $Q^{\rm POST}-Q^{\rm PRE}$ [inset in Fig. 2(b)] is consistent with zero, we use $Q^{\rm PRE}=Q^{\rm HE}=Q^{\rm POST}$. The weighted average for the target polarization over all runs below 450 MeV, including both, the ''PRE'' and the ''POST'' measurement, is given in the inset in Fig. 2(a). The analogous treatment of the separate 450 MeV data set leads to a target polarization of $Q(450\ {\rm MeV})=0.730\pm 0.0.013$.

C. Beam polarization loss during acceleration or deceleration

The relative change of the beam polarization during acceleration, $P^{\rm HE}/P^{\rm PRE}$, can be deduced from the measured asymmetries by forming the double ratio $\{p_i^{\rm HE}\|q_i^{\rm HE}\}/\{p_i^{\rm PRE}\|q_i^{\rm PRE}\}$ which equals $(P^{\rm HE}/Q^{\rm HE})/(P^{\rm PRE}/Q^{\rm PRE})$ (because the analyzing powers cancel) which in turn equals $P^{\rm HE}/P^{\rm PRE}$ (because $Q^{\rm HE}=Q^{\rm PRE}$). The same procedure is used to deduce $P^{\rm POST}/P^{\rm HE}$, the relative change during the down ramp. Note, that this method does not require the knowledge of the analyzing power of the reaction.

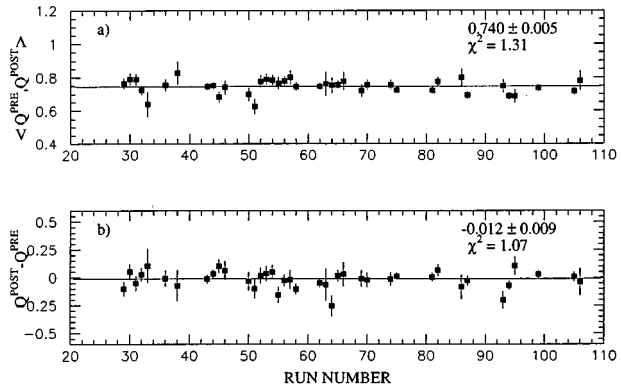

FIG. 2. (a) Average of the target polarizations Q^{PRE} before, and Q^{POST} after the two energy ramps as a function of run number. The measurements extend over a period of about a week. The inset numbers are the weighted averages over all measurements, and the respective χ^2 per degree of freedom. (b) Shows the difference Q^{POST}-Q^{PRE}, illustrating that the target polarization is constant throughout the cycle. Only the statistical errors are shown.

For this study, data at a given accelerated energy T' are analyzed together, resulting in a single datum per T' in Fig. 3. A ratio of less than one indicates polarization loss. With the exception of the 450 MeV point (open symbol in Fig. 3) which was from a different running period, the polarization loss data for all energies T' are consistent with each other. This can be explained by noting that magnet ramps to different energies T' are all similar near the injection energy; this energy is also the one closest to the intrinsic depolarization resonance (see Sec. II). The weighted averages over the data at all T' (excluding the 450 MeV datum) are $\epsilon_1 = \langle P^{\mathrm{HE}}/P^{\mathrm{PRE}}\rangle = 0.988 \pm 0.009$, and $\epsilon_2 = \langle P^{\mathrm{POST}}/P^{\mathrm{HE}}\rangle = 0.972 \pm 0.009$. From Fig. 3 it can be seen that a significant beam polarization loss is observed only for the down ramp. The corresponding values for ϵ_1 and ϵ_2 at 450 MeV are represented by the open symbol in Fig. 3. It should be pointed out that for the present analysis we have assumed a Gaussian probability distribution for all quantities which, strictly speaking, is not quite true because during a ramp polarization can be lost but never gained.

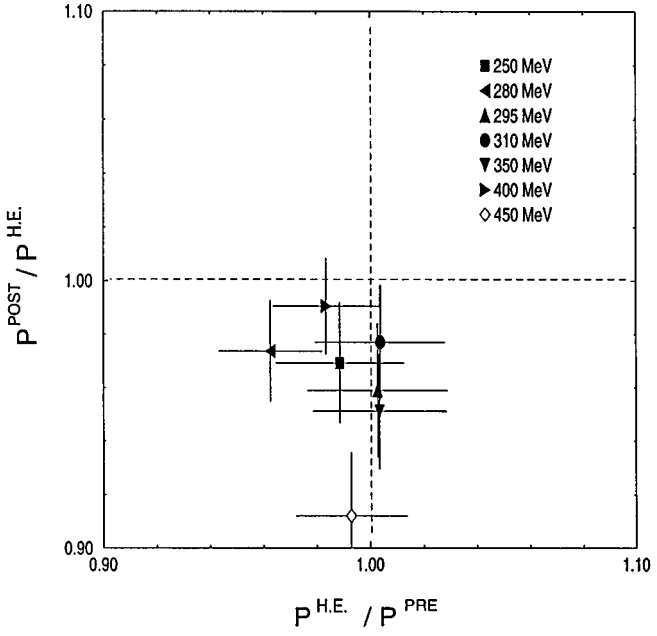

FIG. 3. Ratio of the beam polarization before and after each of the two energy ramps, for the up ramp (horizontal axis), and the down ramp (vertical axis). Only the statistical errors are shown. The data are grouped with respect to the energy T' after acceleration (see inset). A ratio of less than one indicates polarization loss. The measurements show a significant polarization loss only for the down ramp. Data with solid symbols have all been acquired during the same running period.

Based on these findings we conclude that the beam polarization change during the up and down ramps combined, is given by $P^{\mathrm{POST}} = \epsilon_1\epsilon_2 P^{\mathrm{PRE}}$, where $\epsilon_1\epsilon_2 = (0.960 \pm 0.012)$. This relation is applicable for all of the data, except those at 450 MeV where the values for ϵ_1 and ϵ_2 determined at just that energy were used.

D. Beam polarization

We do not expect the beam polarization in the ring to be constant for the whole experiment. This is in part because of slow changes in the performance of the ion source that supplies the polarized beam, and in part because the beam polarization somewhat depends on the number of cycles for which the beam has been accumulated [10]. Thus, the beam polarization must be determined for each energy T' individually. Using the same method as described in Sec. IV B, the beam polarization was deduced from the average of the ratios $\epsilon_1\{p_j^{\mathrm{PRE}} \| a_j^{\mathrm{cal}}\}$ and $\{p_j^{\mathrm{POST}} \| a_j^{\mathrm{cal}}\}/\epsilon_2$. Values between 0.52 and 0.63 were found for $P(T')$.

E. Establishing a new polarization standard

An analyzing reaction at a new energy T' can become a new standard because it is possible to calibrate the beam polarization (method A), or the target polarization (method B) at that energy.

The target polarization has been found to be constant during a full cycle, as well as during the whole run (see Sec. IV B). For the beam polarization we have found that the loss during acceleration is close to zero, $(1.2 \pm 0.9)\%$. Moreover, we have deduced a value for the polarization loss between the ''PRE'' and ''POST'' measurements at the calibration energy T_0. However, the beam polarization changes over the course of the experiment, and thus only the runs at a given T' can be used to determine the beam polarization at that T'. Consequently, the statistical error of P^{HE} is larger than for Q^{HE} which is based on a larger set of data.

The data acquired in this experiment allow a comparison of the methods A and B. To this aim, consider for a moment the ratio of the asymmetry distributions $\{q_i^{\mathrm{HE}} \| q_i^{\mathrm{PRE}}\}$ (see Sec. IV A). In this ratio the target polarization Q cancels, leaving the ratio of the analyzing powers, $\{A_y(T',\theta_i) \| A_y(T_0,\theta_1)\}$. Even though the two A_y distributions are for different energies and, in general, do not have the same shape, this ratio is still defined and is given entirely by the properties of the reaction at T_0 and T'.

In the following, we deduce this ratio from the data using either the polarized beam or the polarized target. This

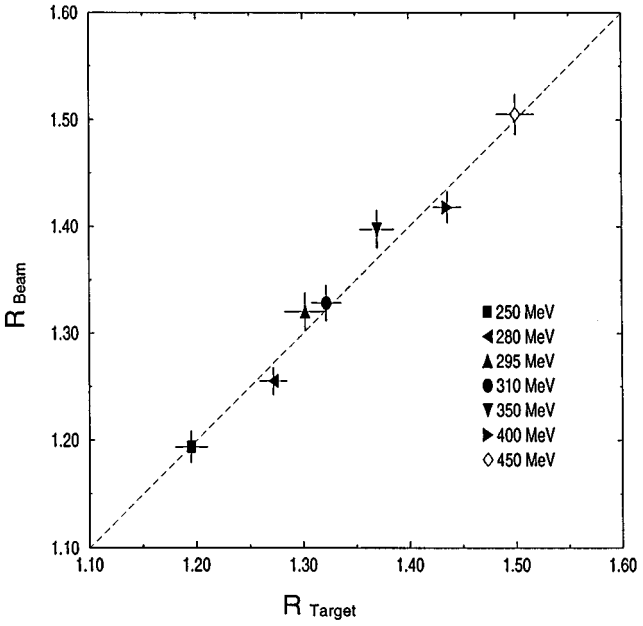

FIG. 4. The distribution ratios R_{beam} and R_{target} as defined in Eq. (2) for the seven beam energies T' (see inset) covered in this experiment. Each of the two numbers is expected to yield the analyzing power distribution ratio $\{A_y(T',\theta_i)\|A_y(T_0,\theta_i)\}$, given entirely by the properties of the reaction at T_0 and T'. Thus, the equality of R_{beam} and R_{target} demonstrates the consistency of the calibration methods A and B. Only the statistical errors are shown.

amounts to a consistency check of the two methods A and B. Here, we combine the data at the injection energy by taking the bin-by-bin average of the asymmetry distributions from both, the ''PRE'' and the ''POST'' phase. Thus, we evaluate the following statistically independent distribution ratios:

$$R_{\text{targ}_{\text{et}}}=\{q_i^{\text{HE}}\|\tfrac{1}{2}(q_i^{\text{PRE}}+q_i^{\text{POST}})\},$$

$$R_{\text{beam}}=\left\{\frac{1}{\epsilon_1}\,p_i^{\text{HE}}\|\frac{1}{2}\left(p_i^{\text{PRE}}+\frac{1}{\epsilon_1\epsilon_2}\,p_i^{\text{POST}}\right)\right\}. \qquad (2)$$

In the evaluation of R_{beam}, use has been made of the measured (small) beam depolarizations ϵ_1 and ϵ_2, incurred during the energy ramps. Figure 4 shows the result of this study for the seven different energies T', demonstrating that the methods A and B are indeed consistent.

For the special case of this experiment, information from both methods (A and B) will be combined to establish a polarization standard at the new energies T. The result will take the form of analyzing powers and spin correlation coefficients for pp elastic scattering at seven energies between 250 and 450 MeV. These data will be the subject of a forthcoming paper.

V. DISCUSSION AND CONCLUSIONS

A. Export of the polarization standard

We have discussed two methods to export a polarization standard from one energy to another. Method A makes use of a polarized beam, while method B requires a polarized target. In both methods a polarization standard is used to establish the polarization of the beam (or the target) at some energy T_0. After the energy change, the absolute polarization of the beam (or the target) is still known, making possible the absolute measurement of an analyzing reaction. The two methods have the following limitations.

Method A only works if the beam polarization during the ramp to a new energy and back does not change appreciably. If there is a loss of polarization, it is not known *a priori* if it is incurred before or after the measurement at the new energy; the difference in this case must be treated as an uncertainty. In the example presented in this paper, no significant beam polarization loss was found during acceleration. In general, for large energy changes where depolarizing resonances must be crossed, it is difficult to keep polarization losses negligible. However, it has been shown by a measurement at SATURNE II [12] that, even in this case, the method is useful to determine the beam polarization at the higher energy, since the polarization lost when crossing resonances can be made the same for acceleration and deceleration.

Method B requires the technical effort of an internal polarized target. Moreover, it is only applicable to establishing the analyzing power of reactions that either involve a polarized target, or for which it is technically and kinematically feasible to reverse the roles of beam and target.

B. Systematic errors

Method A involves a measurement of the beam polarization at the injection energy T_0 before and after the excursion to the higher energy. It is of course necessary that the beam energies for the two measurements are the same. Moreover, the absolute beam energy has to be known in order to match the energy of the calibration standard. The beam energy in our case is determined from the beam-bunching rf frequency and the known ring circumference. The circumference has been calibrated using the accurately known threshold energy of pion production reactions [11]. Consistent values for the ring circumference have been deduced from data taken at different times, indicating that it is difficult to change the length of the closed orbit. Typically, the uncertainty of the absolute beam energy is a few hundred keV. This figure needs to be compared with the energy dependence of the pp analyzing power near 200 MeV of about 0.5% per MeV.

The measured asymmetries in the three data taking phases (''PRE,'' ''HE,'' and ''POST'') can be caused in part by instrumental asymmetries. The latter can arise, for instance, from a transverse displacement or a change of angle of the beam on the target. In the experiment described here, beam position and angle are actually measured with an accuracy of ± 0.1 mm and 0.05°, respectively. Beam shifts of the order of 1 mm have been observed between the ''PRE'' and ''HE'' and ''POST'' phases. However, in the analysis of the data, allowance is made for these shifts. A Monte Carlo simulation is used to demonstrate that the remaining effect of beam shifts, including those that are correlated to the target guide field, on the measured asymmetries is negligible (for more detail, see Ref. [3]).

Method A assumes that the direction of the beam polarization at T_0 and at T' is the same (in this case: vertical). Nonvertical fields in the ring lattice could, in principle, cause the stable direction of the stored polarization to deviate from

vertical. It is then likely that this deviation is different at the two energies. However, the undesired transverse and longitudinal components of the beam polarization are actually measured in this experiment (via the knowledge of the spin correlation coefficients), and found to be consistent with zero. Since, for instance, a change of a nonvertical component of about $\Delta P_{\mathrm{nonvert}}=0.1$ would imply only a change of 1% in the vertical component, this systematic error is negligible.

C. Consequences of deceleration

The capability of decelerating the beam energy has been developed to be able to apply method A. However, there is another benefit from deceleration which we would like to mention here.

A measurement which calls for accelerated beam implies that injection conditions are reestablished at the beginning of every cycle. If it is possible to decelerate, the beam which is still stored at the end of the cycle can be preserved. This is especially important if the beam loss during the cycle is small (which is the case for the relatively thin polarized target which is used in this study). The gain from the deceleration is the ratio of the time-averaged luminosities for the two cases when the beam is either kept or discarded at the end of the cycle. The gain depends on many factors, such as the beam lifetime, the fill rate, and the beam loss during the energy ramps. In the present experiment, gain factors of between 3 and 6 have been observed.

ACKNOWLEDGMENTS

The authors would like to thank G. East, B. Manwaring, and T. Sloan for devoting their expertise and a lot of patience to developing the deceleration capability for the Indiana Cooler. One of us (F.R.) would like to thank the Alexander von Humboldt Foundation for their generous support. This work has been supported by the U.S. National Science Foundation under Grant Nos. NSF PHY 93-14783 and NSF PHY 93-16221.

[1] B. v. Przewoski, H. O. Meyer, P. V. Pancella, S. F. Pate, R. E. Pollock, T. Rinkel, F. Sperisen, and J. Sowinski, Phys. Rev. C **44**, 44 (1991).
[2] S. W. Wissink *et al.*, Phys. Rev. C **45**, R504 (1992).
[3] W. Haeberli *et al.*, Phys. Rev. C **55**, 597 (1997).
[4] F. Rathmann *et al.* (unpublished).
[5] X. Pei, Ph.D. thesis, Indiana University, 1991 (unpublished).
[6] B. J. Hamilton, M. S. Ball, and T. J. P. Ellison, Nucl. Instrum. Methods Phys. Res. A **342**, 314 (1994).
[7] W. A. Dezarn *et al.*, Nucl. Instrum. Methods Phys. Res. A **362**, 36 (1995).
[8] M. A. Ross *et al.*, Nucl. Instrum. Methods Phys. Res. A **344**, 307 (1994).
[9] D. D. Caussyn *et al.*, Phys. Rev. Lett. **73**, 2857 (1994).
[10] B. v. Przewoski *et al.*, Rev. Sci. Instrum. **67**, 165 (1996).
[11] H. O. Meyer, C. Horowitz, H. Nann, P. V. Pancella, S. F. Pate, R. E. Pollock, B. v. Przewoski, T. Rinkel, M. A. Ross, and F. Sperisen, Nucl. Phys. A **539**, 633 (1992).
[12] J. Bystricky *et al.*, Nucl. Instrum. Methods Phys. Res. A **234**, 412 (1985).